Revista Facultad de Ingeniería
Journal Homepage: https://revistas.uptc.edu.co/index.php/ingenieria

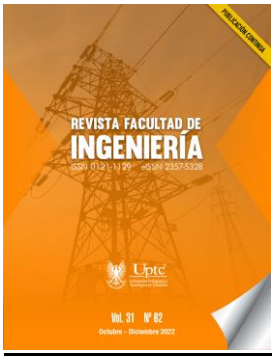

Wear Behavior of Bioactive Glass Coatings Deposited by Thermal Spraying

Mónica-Johanna Monsalve-Arias[1]
Oscar-Fabián Higuera-Cobos[2]
Helèn Ageorges[3]
Fabio Vargas-Galvis[4]
María-Esperanza López-Gómez[5]

Received: August 23, 2022 **Accepted:** October 25, 2022 **Published:** November 01, 2022

Citation: M.-J. Monsalve-Arias, O.-F. Higuera-Cobos, H. Ageorges, F. Vargas-Galvis, M.-E. López-Gómez, "Wear Behavior of Bioactive Glass Coatings Deposited by Thermal Spraying", *Revista Facultad de Ingeniería*, vol. 31 (62), e14778, 2022. https://doi.org/10.19053/01211129.v31.n62.2022.14778

[1] Ph. D. Universidad Nacional de Colombia (Bogotá-Distrito Capital, Colombia). momonsalvea@unal.edu.co. ORCID: 0000-0002-9902-8518
[2] Ph. D. Universidad del Atlántico (Barranquilla-Atlántico, Colombia). oscarhiguera@mail.uniatlantico.edu.co. ORCID: 0000-0002-4836-5215
[3] Ph. D. University of Limoges (Limoges, France). helene.ageorges@unilim.fr. ORCID: 0000-0003-1302-0388
[4] Ph. D. Universidad de Antioquia (Medellin-Antioquia, Colombia). fabio.vargas@udea.edu.co. ORCID: 0000-0003-4484-3950
[5] Ph. D. Universidad de Antioquia (Medellín-Antioquia, Colombia). esperanza.lopez@udea.edu.co. ORCID: 0000-0002-1038-6504

Abstract

In this work, bioactive glass coatings were fabricated by plasma thermal spraying and oxyacetylene flame techniques from 2 different bioactive glass powders with 0 and 2% molar MgO. The metal substrates used were Ti6Al4V alloy and AISI 316L steel. The tribological behavior of the coatings was evaluated by the ball-on-disc method in the presence of simulated biological fluid (SBF), and the results were correlated with their mechanical behavior, obtaining values of hardness (between 4.84 and 5.18 GPa) and fracture toughness (between 5.25 and 6.62 MPa.m1/2). The results show that fracture toughness has a slightly higher effect than hardness on the wear behavior of the coatings under study.

Keywords: bioactive glass; ceramics; coatings; flame spraying; plasma spraying.

Comportamiento al desgaste de recubrimientos de vidrios bioactivos depositados por proyección térmica

Resumen

En este trabajo se fabricaron recubrimientos de biovidrio mediante las técnicas de proyección térmica por plasma y por llama oxiacetilénica a partir de 2 polvos de biovidrio diferentes con 0 y 2% molar de MgO. Los sustratos metálicos utilizados fueron una aleación Ti6Al4V y un acero AISI 316L. El comportamiento tribológico de los recubrimientos se evaluó mediante el método ball-on-disc en presencia de fluido biológico simulado (SBF) y los resultados se correlacionaron con los de su caracterización mecánica realizada midiendo su dureza (con valores entre 4.84 y 5.18 GPa) y resistencia a la fractura (con valores entre 5.25 y 6.62 MPa.m1/2). Los resultados muestran que la tenacidad a la fractura tiene un efecto ligeramente superior a la dureza sobre el comportamiento al desgaste de los recubrimientos en estudio.

Palabras clave: biovidrio; cerámicos; proyección térmica por llama oxiacetilénica; proyección térmica por plasma; recubrimientos.

Comportamento ao desgaste de revestimentos de vidro bioativo depositados por projeção térmica

Resumo

Neste trabalho, revestimentos de biovidro foram fabricados usando técnicas de pulverização térmica de plasma e oxiacetileno a partir de 2 pós diferentes de biovidro com 0 e 2 mol% de MgO. Os substratos metálicos utilizados foram uma liga Ti6Al4V e um aço AISI 316L. O comportamento tribológico dos revestimentos foi avaliado pelo método ball-on-disc na presença de fluido biológico simulado (SBF) e os resultados foram correlacionados com os de sua caracterização mecânica realizada medindo sua dureza (com valores entre 4,84 e 5,18 GPa) e resistência à fratura (com valores entre 5,25 e 6,62 MPa.m1/2). Os resultados mostram que a tenacidade à fratura tem um efeito ligeiramente maior do que a dureza no comportamento ao desgaste dos revestimentos em estudo.

Palavras-chave: biovidro; cerâmica; projeção térmica por chama de oxiacetileno; revestimentos; spray térmico de plasma.

I. Introduction

Every year, two million people worldwide suffer from illnesses or trauma due to accidents, and many undergo hip and knee prostheses, achieving a considerable improvement in their quality of life [1]. For decades, bioactive glass has been proposed as an alternative to solve some orthopedic problems, such as segmental bone replacements and the fixation of hip prostheses, thanks to the bonding to the bone through the formation of a surface-active calcium-phosphate interface. To achieve the performance required for use in hip prostheses, bioactive glass has been applied as a coating to metal and ceramic substrates [2] [3].

Metal implants coated with bioactive glass have the advantage of the bioactivity of the coatings and the mechanical strength of the substrates [4] [5]. Since these coatings are widely used to facilitate and improve the fixation and integration of orthopedic implants [6], their tribological performance is important when they are in contact in relative movement with bone or other material. The relative movement can generate particles from the worn material, which will be phagocytized by macrophages into the surrounding tissue, eventually leading to inflammation, bone reabsorption, aseptic loosening and perhaps a revision of surgery [7] [8] [9]. In this paper, the wear resistance of two bioactive glass coatings deposited by flame and plasma spraying on Ti6Al4V and stainless steel AISI 316L substrates were studied.

II. Materials and Methods

A. Characterization of Powders

Two batches of calcium oxide, silicon oxide, phosphorus oxide, and magnesium oxide, all of reagent grade (Alfa Aesar), were mixed, melted, and milled to produce glass powders. The mixed oxides were placed in a platinum crucible and heated in an electric furnace at 1600 °C for three h at a heating rate of 9 °C/min. Then, the melted material was quenched in water to obtain a frit. The frit was ground in a tungsten carbide ball milling machine and subsequently sieved to obtain particles smaller than 67 µm. The chemical composition of the glass powders obtained was determined by wave-dispersive X-ray fluorescence spectrometry using a Thermo

Scientific ARL OPTIM'X XRF Analyzer. The particle size distribution of the powders was measured by laser diffraction with a Master Sizer 2000 instrument. The chemical composition and distribution size particle of the obtained powders are given in Table 1.

Table 1. Chemical composition and distribution size particle of the synthesized glass powders.

Code	SiO_2, wt% (%molar)	CaO, wt% (%molar)	MgO, wt% %molar)	P_2O_5, wt% (%molar)	Others, wt%	% Crystallinity	Size particle		
							D_{10}	D_{50}	D_{90}
F1	28.0 (31)	48.3 (58)	0.14 (0)	22.9 (11)	0,66	2.56	8.8	32.1	66.2
F2	28.3 (31	47.3 (56)	1.40(2)	23 (11)	-----	2.43	5.1	27.9	61.6
P1	27.2 (31)	49.4 (58)	0.2 (0)	22.7 (11)	0.42	66.44	13.3	31	59.1
P2	28.8 (31)	45.6 (56)	1.3 (2)	24.2 (11)	0.07	45.71	1.8	15	39.7

The percentage of crystalline phases in the powders and coatings was determined by X-ray diffraction (XRD) using a Bruker D8 Advance diffractometer with a copper radiation source (CuKa, λ = 1.5418 Å) operated at 40 kV and 30 mA and calculated using the HighScore Plus software.

B. Manufacture of Coatings

Coatings from glass of 31SiO2-11P2O5-(58-X)-CaO-XMgO system, with X=0 and X=2 were manufactured by atmospheric plasma spraying and flame spraying on AISI 316 L stainless steel and Ti6Al4V substrates, respectively. Previously to the deposition of coatings, specimens with 19 mm in diameter and 5 mm in height were machined for substrates, using both Ti6Al4V and AISI 316L SS bars. The substrates were grit blasted with corundum particles and subsequently cleaned in an ultrasonic bath using ethanol, reaching an arithmetic average of the surface roughness (Ra) ≈ 5 µm.

The plasma for the APS (Atmospheric plasma spraying) process was obtained by applying 650 A at 60 V to a mixture of Ar/H2, 47/8 L/min in a Sulzer MetcoF4MB torch. The substrates were preheated with the plasma jet to 300 ºC, and then each glass powder was sprayed using 9 L/min of argon as carrier powder gas. The spray

distance was 60 mm. On the other hand, a Eutectic-Castolin Terodyn 2000 torch was fed with acetylene and oxygen with a C2H2:O2 of 22:38 L/min ratio to manufacture the coatings by flame spraying process. The substrates were preheated by the oxyacetylene flame to 280 °C, and subsequently, each glass powder was sprayed using 17 L/min of nitrogen as the carrier gas, with a spraying distance of 80 mm. The samples were coded according to the spraying process and the MgO molar content. The plasma-sprayed coatings from powders with 0 and 2 molar percentage were coded as P1 and P2, respectively, while those sprayed by flame using glass powders with 0 and 2 molar percentage were codified as F1 and F2, respectively.

C. Characterization of Powders

The obtained bioactive glass powders show an angular morphology characteristic of ceramics produced by milling processes (see Figure 1). The particle sizes ranged between 1.8 and 66.2 µm, being F2 and P2 particles smaller than those of F1 and P1 powders.

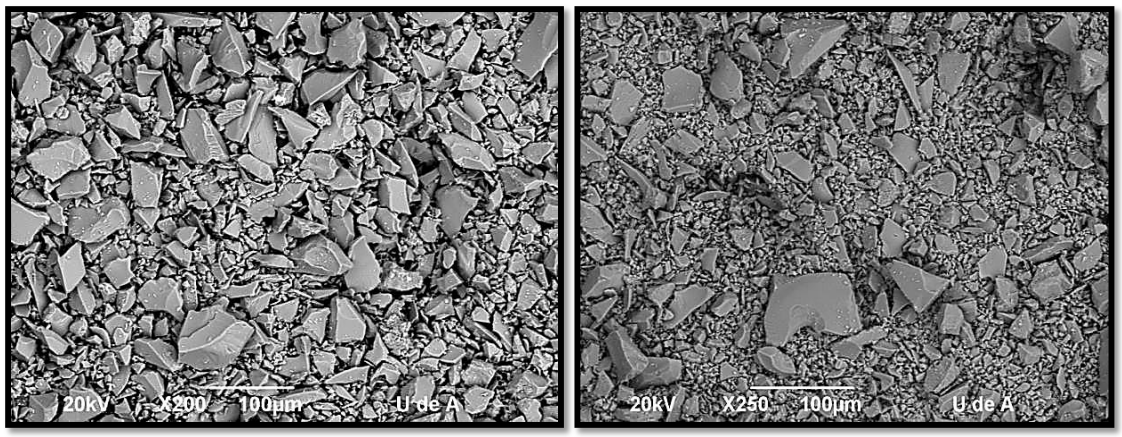

Fig. 1. SEM micrographs of glass powders. (a) P1 y (b) F1.

D. Characterization of Coatings

1) Structure and Mechanical Properties. The structure and mechanical properties of the coatings were evaluated on their cross-section. To evaluate the structure and

mechanical properties of the coatings, the samples were embedded in resin, cut, and polished according to ASTM E1920 standard [10]. Subsequently, the structure of the coatings was analyzed using a JEOL JSM-6490LV Scanning Electron Microscope (SEM). The structural defects of the coatings were quantified by image analysis using the free software ImageJ, for which 25 images were obtained at 100 magnifications in an Olympus BX41 Optical Microscope for each sample and analyzed according to the ASTM E2109 standard [11], the thickness of the coatings was assessed along of their cross-section by analyzing images obtained by scanning electron microscopy (JEOL JSM-6490LV). On the other hand, the mechanical properties, microhardness, and fracture toughness were calculated from the indents produced by a Vickers indenter using a Wilson Instruments and an Instron Company Model 401MVD equipment, respectively. To determine the microhardness of the coatings, 25 measurements were carried out to each one applying on the indenter a load of 100 g-f (0.98N) for 15 seconds, according to the ASTM C1327 standard [12]. As for the fracture Toughness, this was calculated from the maximum radial crack length (C), measured from the center of the Vickers indent, for which 25 indentations were performed applying a load (P) of 200 g-f on the indenter for 15 seconds. Since Vickers indentation results are not appropriate to calculate the fracture toughness (Kc) of ceramic materials from glassy materials, this property was calculated from the P/C ratio according to eq. (1) [13].

$$K_c = \frac{0.0515P}{C^{3/2}} \quad (1)$$

2) Wear Behavior. Wear resistance was measured with a ball-disc tribometer using an alumina ball 6 mm in diameter as a counter-body whose Vickers Hardness is 19 ± 0.3 GPa, as shown in Figure 2. The test was performed at atmospheric pressure and 37°C in the presence of the simulated biological fluid (SBF) proposed by Kokubo [14].

Fig. 2. Assembly used to perform tribological tests.

The load used was 2.46 N, and the test duration was 2.5 h at 139 rpm during 20,880 cycles. Before starting the test, the surface of the coatings was polished to a roughness average (Ra) ±0.4 µm. The morphology of the surface of the assayed sample was observed by scanning electron microscopy. The wear rate was calculated using eq. (2) [15].

$$\text{Wear rate} = \frac{\text{volume of wear}}{\text{Load x sliding distance}} = \frac{S_T 2\pi r}{P 2\pi r N_c 1000} \qquad (2)$$

Where: ST= Groove area caused by wear (µm2); Nc= Number of cycles performed during the test; P= normal load applied (N); r = radius of the circular track produced by the friction of the ball on the disc (mm). Table 2 shows the values used to calculate the wear rate.

Table 2. Values used in the calculation of the wear rate.

	Plasma spraying		**Flame spraying**	
	0HP	**2HP**	**0HF**	**2HF**
Coating roughness before the test (µm)	0.39	0.42	0.31	
Load (N)	2.46		2.46	
Sliding distance (m)	590		761	997
Number of cycles performed during the test	20,880		20,880	
Time (h)	2.5 h		2.5 h	

DOI: https://doi.org/10.19053/01211129.v31.n62.2022.14778

III. Results and Discussion

A. Structural Characterization of Coatings

The structure of the cross-section of coatings is shown in Figure 3, and their thickness is presented in Table 3. All coatings showed cracks perpendicular and parallel to the interface between the coating and the substrate, which are more evident in the plasma-sprayed coatings (Figures 3a and 3b). Perpendicular cracks are caused by residual stresses generated during the coating cooling, while cracks parallel to the substrate surface are associated with problems at the lamella interfaces [16]. In addition, pores and non-melted particles were observed in the coatings' structure. The percentage of these microstructural defects was higher in the technique by flame spraying (Figures 3c and 3d) than in the coatings manufactured by the plasma process (Table 3). This is caused by the fact that both the temperature of the flame and the speed at which the particles are sprayed are lower than those of plasma Sputtering.

Table 3. Results of structural, mechanical and tribological characterization of coatings.

	0HP	**2HP**	**0HF**	**2HF**
Thickness [µm]	263	403	271	297
Crystallinity of the starting powders	66.44	45.71	2.56	2.43
CaO/SiO_2 ratio of starting powders	1.87	1.81	1.87	1.81
Crystallinity of coatings	37.21	23.17	3.28	2.76
microstructural defects [%]	9.49±0.98	6.34±0.93	20.96±0.81	10.07±0.89
Hardness [GPa]	4.84±0.44	5.18±0.46	5.16±0.67	5.09±0.72
Fracture Toughness [$MPa.m^{1/2}$]	5.25±0.74	5.9±0.87	6.62±1.1	6.31±1.28
Wear rate [$mm^3/N.m$]	$2{,}22x10^{-4}$±$3.06x10^{-5}$	$1{,}45x10^{-4}$±$1.65x10^{-5}$	$2{,}65\ x10^{-6}$±$6.12x10^{-7}$	$1{,}33\ x10^{-6}$±$9.29x10^{-7}$

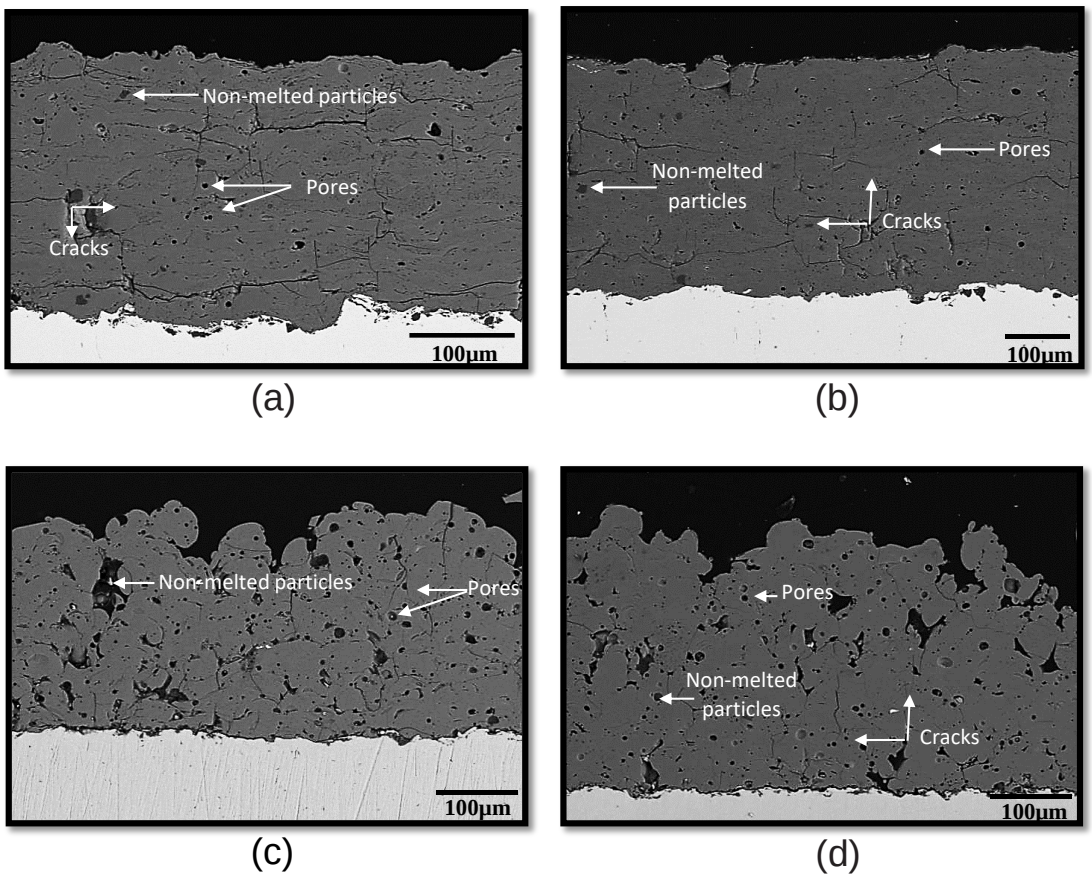

Fig. 3. Cross-section of bioactive glass coatings deposited by plasma and flame spraying. (a) 0HP AISI 316L steel, (b) 2HP AISI 316L steel, (c) 0HF Ti6Al4V and (d) 2HF Ti6Al4V.

Consequently, the sprayed particles reach a lower temperature and speed before impacting the substrate, producing stacking failures, which increases the porosity in the structure of coatings. In general, coatings have good adhesion with the substrate, being better those manufactured by plasma spraying.

B. Mechanical Properties and Tribological Performance

The results of the hardness and fracture toughness of coatings are shown in Table 3. The hardness values for coatings deposited by both techniques are statistically similar, while those of cracking resistance are slightly higher for the coatings manufactured by the flame spraying process. The flame-sprayed coatings have a higher percentage of pores but a lower quantity of vertical and parallel cracks in their structure, which may prevent the generation and propagation of cracks during

indentation tests. On the other hand, the analysis of the wear tracks produced on the coatings' surface by sliding contact with the alumina ball revealed the formation of a layer constituted by small particles of glass (Figure 4).

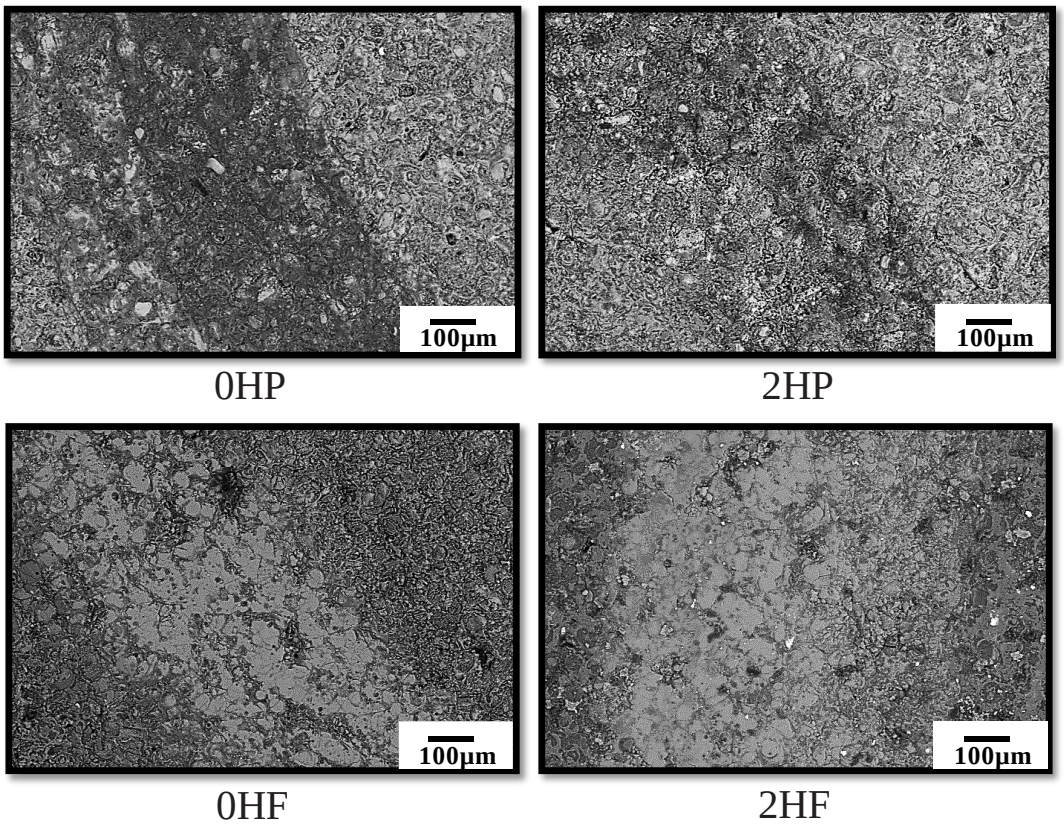

Fig. 4. SEM micrograph of the wear tracks.

In general, the layers formed on each coating show plastic flow. Additionally, they are more continuous in samples sprayed by flame than in those manufactured by the plasma process, and they are even more continuous for coatings manufactured from powders with 2 MgO molar %. The presence of both, SBF and small wear debris, on the friction tracks reduces the contact stresses. Consequently, the layer formed can act as a protective barrier [17] [18] [19].

The plastic flow produced on the layer formed and the absence of large holes produced by particles detached on the wear tracks of the coatings indicate that they withstand the energy applied by sliding contact with the alumina ball and, consequently, a slight wear by ductile deformation was produced [20]. The wear rate

produced in each coating is presented in Table 3. The lower wear rate produced in coatings manufactured by flame spraying is due to their greater cracking resistance and the higher porosity in their structure. The pores in the surface of coatings retain the small particles released from the wear track promoting the formation of a continuous and protective layer.

A statistical analysis was carried out to determine the effect of hardness and fracture toughness on the wear rate of coatings. By correlating the wear rate and the cracking resistance of the coatings, values of approximately 0.96 with a P-value of 0.039 were obtained, while the coefficient of correlation between hardness and wear rate was 0.66 with a P-value of 0.33 (see Table 4). P-values below 0.05 indicate significantly different correlations from zero, with a confidence level of 95.0 %. The statistical analysis of chi-square and F-test showed that fracture toughness has an effect slightly higher than that of hardness on the wear rate results.

Table 4. Statistical analysis results of the effect of hardness and cracking resistance on wear rate.

	Toughness	**Hardness**
Test F	2.14325E-11	1.16015E-09
Chi-Square test	2.40461E-05	0.00014927
Correlation	-0.95909906	-0.66029518

Alok Kumar et al. [21] studied the wear resistance of Hydroxyapatite (5-20 wt.%)-Titanium compounds. They found hardness did not play a crucial role in determining wear resistance compared to fracture toughness. Comparable behaviors were found in the coatings in this study. Similarly, J. Park et al. [22] manufactured two apatite-wollastonite glass-ceramics in MgO-CaO-SiO2-P2O5-F system, to evaluate their tribological behavior. They found in the first material, apatite and wollastonite, as crystalline phases present with a hardness on the free surface of 650±12 HK. In the second material, they found only apatite as crystalline phase with a hardness of 520± 8 HK. The second material was obtained after removing 0.5 mm from the free surface of the first material by mechanical grinding and polishing. Tribological tests were carried out by pin-on-disc method with a free surface wear rate of 0.75±0.05×10-4 mm3/N.m., which increases gradually as the distance from the free surface

increases. The wear rate reached at 0.5 mm below the free surface was 2.93±0.15×10-4 mm3/N.m. Finally, the authors did not find a correlation between the hardness results of apatite-wollastonite glass ceramics and the wear resistance due to the complexity of the wear processes.

IV. Conclusions

The tribological behavior of four coatings manufactured by plasma and flame spraying from glass of 31SiO2-11P2O5-(58-x) CaO-XMgO system, with X=0 and X=2, were studied.

Since the wear developed was by ductile deformation with a protective layer of debris and low wear rates, then: the hardness and the cracking resistance of all four coatings are enough to withstand the energy applied on their surface in wet conditions with SBF and by sliding contact with an alumina ball almost four times harder than them. However, it was evident that the cracking resistance slightly higher in the coatings manufactured by flame spraying increases their wear resistance substantially.

The bioactive glass coatings exhibit good hardness and fracture toughness despite the number of defects in their microstructure. The slight difference in particle size had an important effect on the mechanical properties of the coatings manufactured by thermal plasma spraying. It was found that the 2HP coating manufactured from P2 powder, which had a smaller particle size than the P1 powder, has better mechanical properties than the 0HP coating manufactured from P1 powder. There was no influence of the chemical composition on the mechanical properties.

In this study, it was found that the values of hardness and fracture toughness of the coatings produced by flame thermal spraying are like those obtained for coatings deposited by plasma, despite the difference in the crystallinity of the starting powders. It can be concluded that from the point of view of mechanical properties, the thermal spraying technique by oxyacetylene flame at low speed is suitable for making coatings of bioactive glasses such as those used in this study.

AUTHOR'S CONTRIBUTION

Mónica-Johanna Monsalve-Arias: Investigation, Formal analysis, Methodology, Writing-original draft, Writing-review and editing.

Oscar-Fabián Higuera-Cobos: Investigation, Formal analysis, Methodology, Writing-original draft, Writing-review and editing.

Helèn Ageorges: Supervision, Methodology, Validation.

Fabio Vargas-Galvis: Supervision, Methodology, Validation.

María-Esperanza López-Gómez: Supervision, Methodology, Validation.

REFERENCES

[1] M. Amaral, C. S. Abreu, F. J. Oliveira, J. R. Gomes, R. F. Silva, "Biotribological performance of NCD coated Si3N4–bioglass composites," *Diamond and Related Materials*, vol. 16, no. 4, pp. 790-795, 2007. https://doi.org/10.1016/j.diamond.2006.12.045

[2] L. Hench, J. Pantano, P. Buscemi, D. Greenspan, "Analysis of bioglass fixation of hip prostheses," *Journal of Biomedical Materials Research*, vol. 11, no. 2, pp. 267-282, 1977.

[3] L. G. de Oliveira et al., "Bioglass Ti coatings: Influence of thermal annealing on the evolution of calcium phosphate formation, phase and morphology," *Journal of Non-Crystalline Solids*, vol. 567, e120926, 2021. https://doi.org/10.1016/j.jnoncrysol.2021.120926

[4] S. Bano, I. Ahmed, D. M. Grant, A. Nommeots-Nomm, T. Hussain, "Effect of processing on microstructure, mechanical properties and dissolution behaviour in SBF of Bioglass (45S5) coatings deposited by Suspension High Velocity Oxy Fuel (SHVOF) thermal spray," *Surface and Coatings Technology*, vol. 372, pp. 229-238, 2019. https://doi.org/10.1016/j.surfcoat.2019.05.038

[5] J. Henao, C. Poblano-Salas, M. Monsalve, J. Corona-Castuera, O. Barceinas-Sanchez, "Bio-active glass coatings manufactured by thermal spray: a status report," *Journal of Materials Research and Technology*, vol. 8, no. 5, pp. 4965-4984, 2019. https://doi.org/10.1016/j.jmrt.2019.07.011

[6] Z. Li, N. W. Khun, X.-Z. Tang, E. Liu, K. A. Khor, "Mechanical, tribological and biological properties of novel 45S5 Bioglass® composites reinforced with in situ reduced graphene oxide," *Journal of the Mechanical Behavior of Biomedical Materials*, vol. 65, pp. 77-89, 2017. https://doi.org/10.1016/j.jmbbm.2016.08.007

[7] M. Latorre, *Recubrimientos biocompatibles obtenidos por proyección térmica y estudio in vitro de la función osteoblástica*, Master Thesis, Universitat de Barcelona, Barcelona, 2007.

[8] J. Cai, C. Miyata, X. Huang, Q. Yang, "Microstructure, bioactivity and wear resistance of sintered composite Co-Cr-Mo/Bioglass® for medical implant applications," *International Journal of Surface Science and Engineering*, vol. 8, no. 2-3, pp. 264-281, 2014.

[9] Y. Chen, X. Wang, L. Xu, Z. Liu, K. D. Woo, "Tribological behavior study on Ti–Nb–Sn/hydroxyapatite composites in simulated body fluid solution," *Journal of the Mechanical Behavior of Biomedical Materials*, vol. 10, pp. 97-107, 2012. https://doi.org/10.1016/j.jmbbm.2012.02.017

[10] E04 Committee, *Guide for Metallographic Preparation of Thermal Sprayed Coatings*, ASTM International, 2014. https://doi.org/10.1520/E1920-03R14

[11] E04 Committee, *Test Methods for Determining Area Percentage Porosity in Thermal Sprayed Coatings*, ASTM International, 2014. https://doi.org/10.1520/E2109-01R14

[12] C28 Committee, *Test Method for Vickers Indentation Hardness of Advanced Ceramics*, ASTM International, 2019. https://doi.org/10.1520/C1327-15R19

[13] F. Sergejev, M. Antonov, "Comparative study on indentation fracture toughness measurements of cemented carbides," Proceedings of the Estonian Academy of Sciences and Engineering, vol. 12, no. 4, pp. 388-398, 2006. https://doi.org/10.3176/eng.2006.4.07

[14] T. Kokubo, H. Takadama, "How useful is SBF in predicting in vivo bone bioactivity?," *Biomaterials*, vol. 27, no. 15, pp. 2907-2915, 2006. https://doi.org/10.1016/j.biomaterials.2006.01.017

[15] F. Vargas, *Elaboration des couches ceramiques epaisses a structures micrometriques et nanometriques par projection thermiques pour des applications tribologiques*, Doctoral Thesis, Université de Limoges, Limoges, Francia, 2010.

[16] C. Cano Valencia, *Recubrimientos cerámicos con aplicación en barreras térmicas y ambientales*, Doctoral Thesis, Universidad Autónoma de Madrid, Madrid, 2008.

[17] J. Park, A. Ozturk, "Effect of TiO2 addition on the crystallization and tribological properties of MgO–CaO–SiO2–P2O5–F glasses," *Thermochimica Acta*, vol. 470, no. 1, pp. 60-66, 2008. https://doi.org/10.1016/j.tca.2008.01.018

[18] D. Franco, H. Ageorges, E. López, F. Vargas, "Tribological performance at high temperatures of alumina coatings applied by plasma spraying process onto a refractory material," *Surface and Coatings Technology*, vol. 371, pp. 276-286, 2019. https://doi.org/10.1016/j.surfcoat.2019.04.058

[19] T. E. Fischer, Z. Zhu, H. Kim, D. S. Shin, "Genesis and role of wear debris in sliding wear of ceramics," *Wear*, vol. 245, no. 1, pp. 53-60, 2000. https://doi.org/10.1016/S0043-1648(00)00465-8

[20] G. W. Stachowiak, A. W. Batchelor, "Wear of Non-Metallic Materials," in *Tribology Series*, vol. 24, pp. 715-771, 1993. https://doi.org/10.1016/S0167-8922(08)70590-X

[21] A. Kumar, K. Biswas, B. Basu, "Fretting wear behaviour of hydroxyapatite–titanium composites in simulated body fluid, supplemented with 5 g l-1 bovine serum albumin," *Journal of Physics D: Applied Physics*, vol. 46, no. 40, e404004, 2013. https://doi.org/10.1088/0022-3727/46/40/404004

[22] J. Park, A. Ozturk, "Tribological properties of MgO–CaO–SiO2–P2O5–F-based glass-ceramic for dental applications," *Materials Letters*, vol. 61, no. 8, pp. 1916-1921, 2007. https://doi.org/10.1016/j.matlet.2006.07.155